Supplementary Information for

Perspective of Structural Flexibility on the Selective Inhibition towards CYP1B1 over CYP1A1 by α-naphthoflavone analogs.

Ying Wang[a], Baichun Hu[b,c], Yupeng Zhang[a], Dong Wang[a], Zhaohu Luo[a], Jian Wang[b,c], Fengjiao Zhang[a,*]

a. Wuya College of Innovation, Shenyang Pharmaceutical University, Shenyang 110016, People's Republic of China

b. Key Laboratory of Structure-Based Drug Design & Discovery of Ministry of Education, Shenyang Pharmaceutical University, Shenyang 110016, People's Republic of China

c. School of Pharmaceutical Engineering, Shenyang Pharmaceutical University, Shenyang 110016, People's Republic of China

Corresponding author: Fengjiao Zhang, E-mail: zhangfengjiao@syphu.edu.cn.

Tel: +86-18624131201 Fax: +86-24-23995403

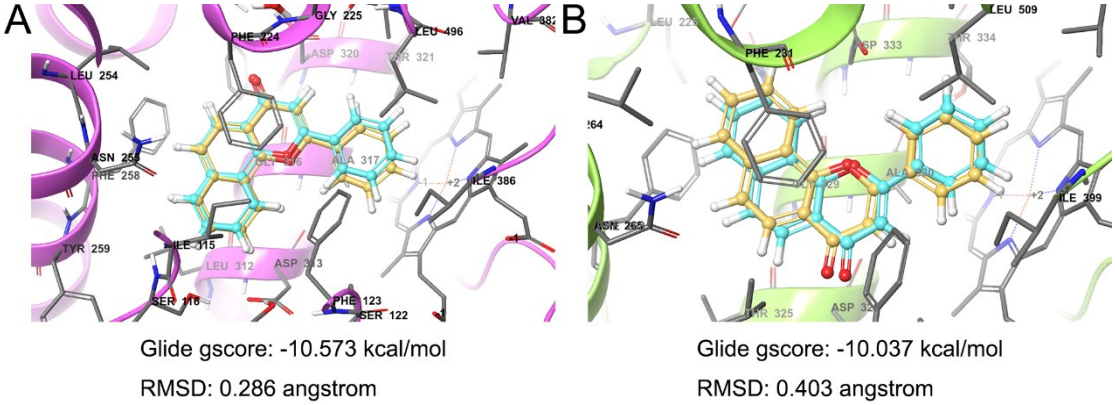

Figure S1 Redocking results of ANF with CYP1A1 and CYP1B1.

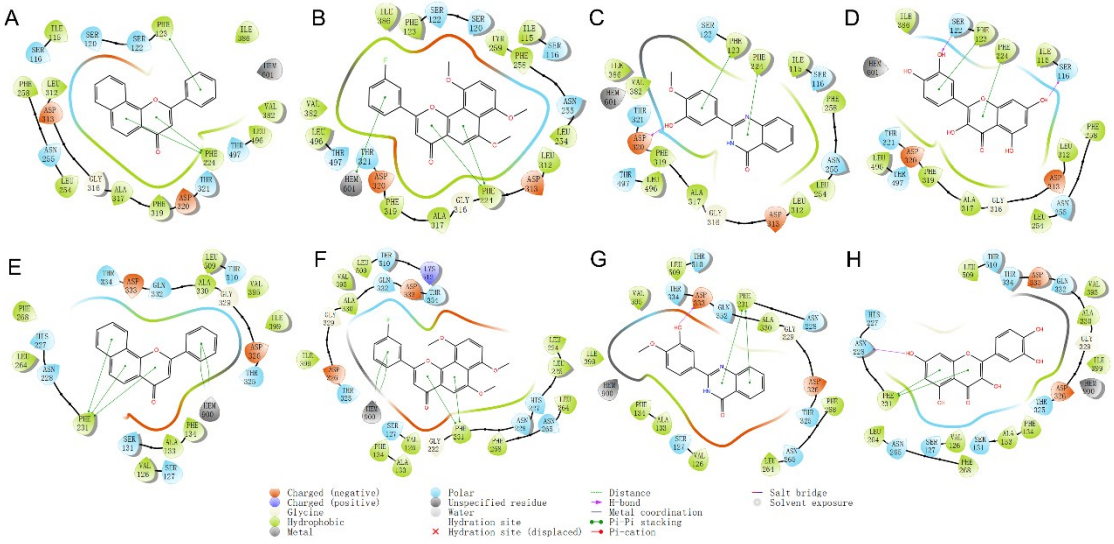

Figure S2 Binding patterns of the investigated selective inhibitors towards CYP1A1 and CYP1B1 minimized by QM/MM methods represented in 2D style. (A) The binding pattern of CYP1A1 and ANF (the crystal structure with PDB code of 4i8v). (B) The binding pattern of CYP1A1 and compound**1**. (C) The binding pattern of CYP1A1 and compound**2**. (D) The binding pattern of CYP1A1 and compound**3**. (E) The binding pattern of CYP1B1 with ANF (the crystal structure with PDB code of 3pm0). (F) The binding pattern of CYP1B1 with compound**1**. (G) The binding pattern of CYP1B1 with compound**2**. (H) The binding pattern of CYP1B1 with compound**3**.

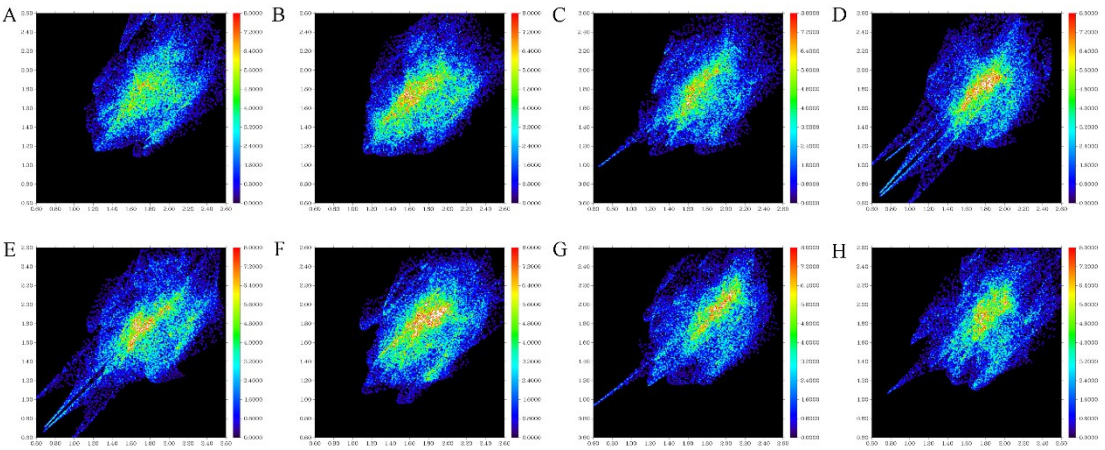

Figure S3 The fingerprint plot of Hirshfeld surface for receptor-ligand interactions. (A) The CYP1A1/ANF complex. (B) CYP1A1/compound**1** complex. (C) The CYP1A1/compound**2** complex. (D) The CYP1A1/compound**3** complex. (E) The CYP1B1/ANF complex. (F) The CYP1B1/compound**1** complex. (G) The CYP1B1/compound**2** complex. (H) The CYP1B1/compound**3** complex. The X axis referred to $d_{i,}$ and the Y axis referred to d_e. The hydrogen bond interactions were denoted as spikes, wherein the upper spikes represented the hydrogen bond donor and the lower spikes represented the hydrogen bond acceptor. The π-π stacking interactions were represented in white.

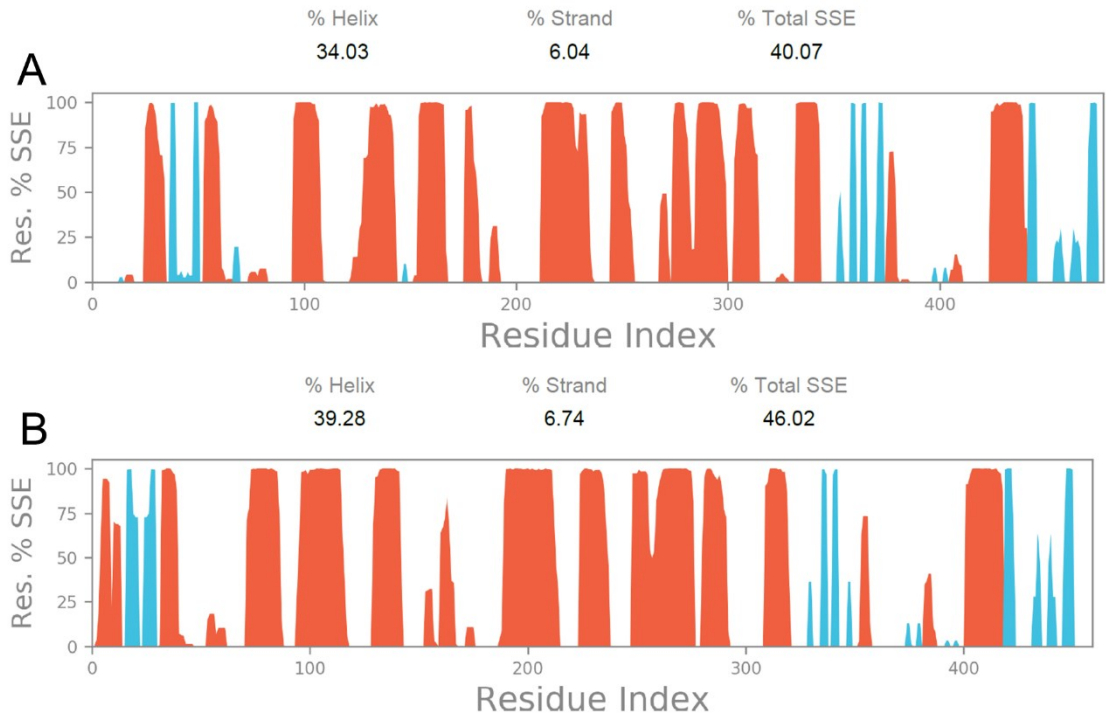

Figure S4 The protein secondary structure elements (SEE) like alpha-helices and beta-strands are monitored throughout the MD simulation for CYP1A1 (A) and CYP1B1 (B).

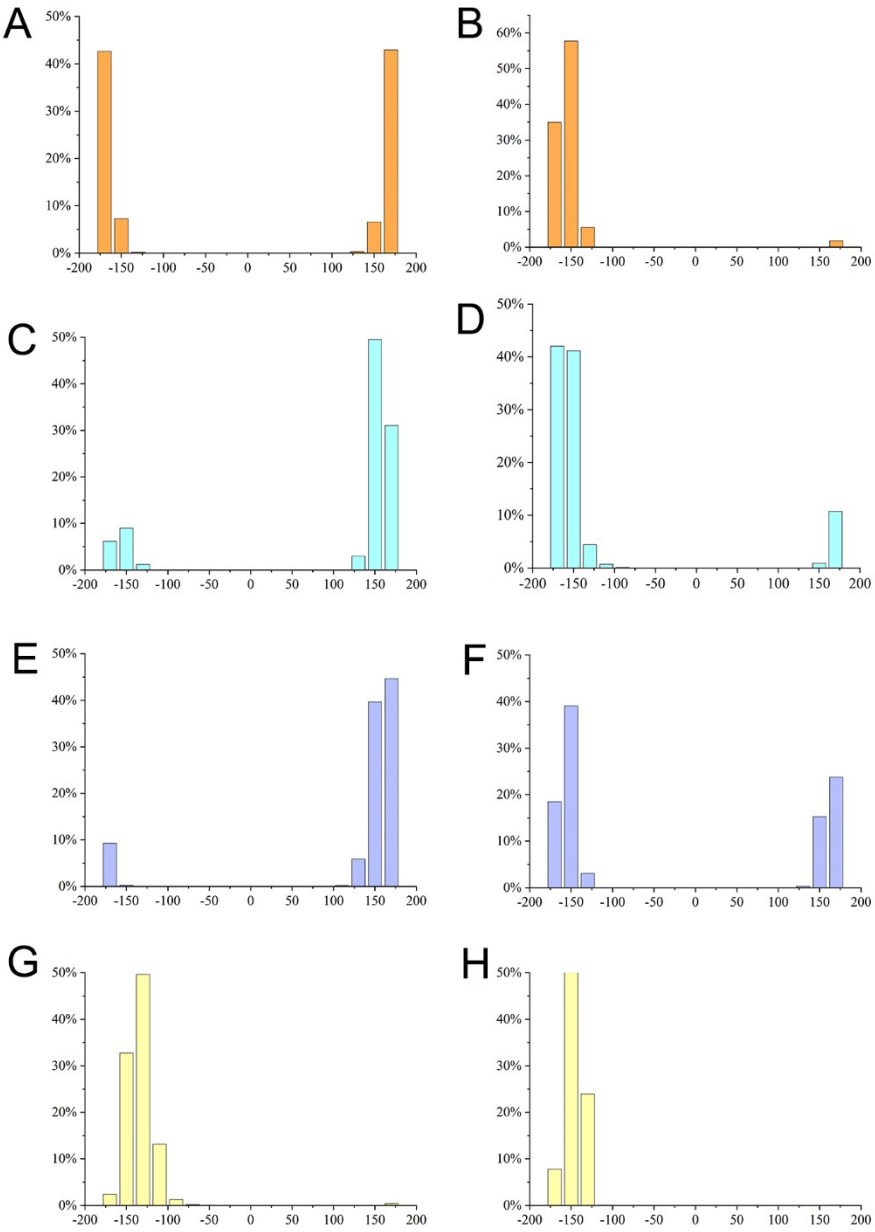

Figure S5 The frequency distribution histogram of the dihedral angle between the B and C ring of each compound throughout the MD simulation for the CYP1A1/ANF complex (A), the CYP1B1/ANF complex (B), the CYP1A1/Compound**1** complex (C), the CYP1B1/Compound**1** complex (D), the CYP1A1/Compound**2** complex (E), the CYP1B1/Compound**2** complex (F), the CYP1A1/Compound**3** complex (G), and the CYP1B1/Compound**3** complex (H).

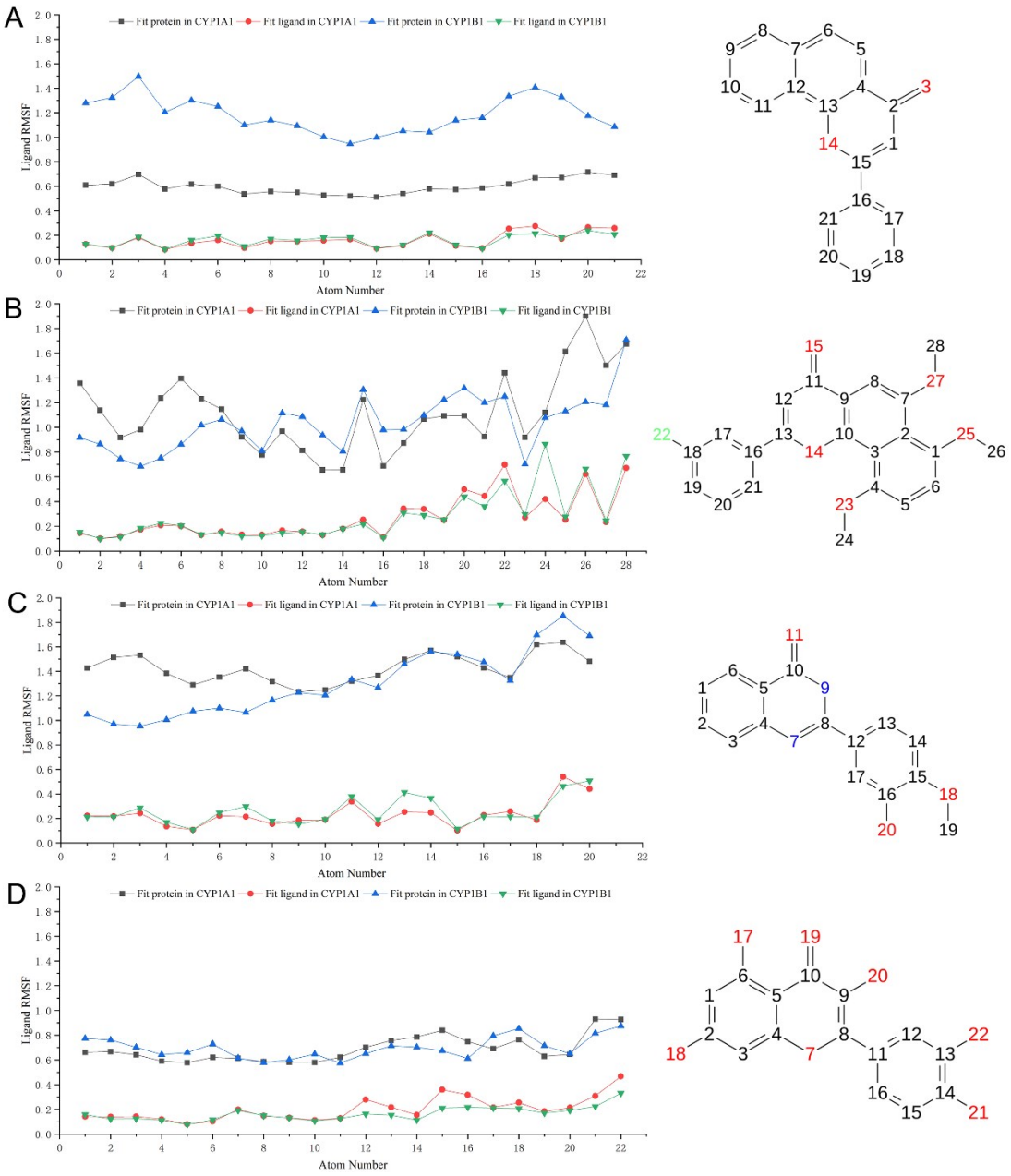

Figure S6 RMSF plots of ligands referring to protein and ligand structures during the MD simulations. The atom number of ligand (left) corresponds to the RMSF plot x-axis (right). (A) ANF, (B) Compound**1**, (C) Compound**2**, (D) Compound**3**.

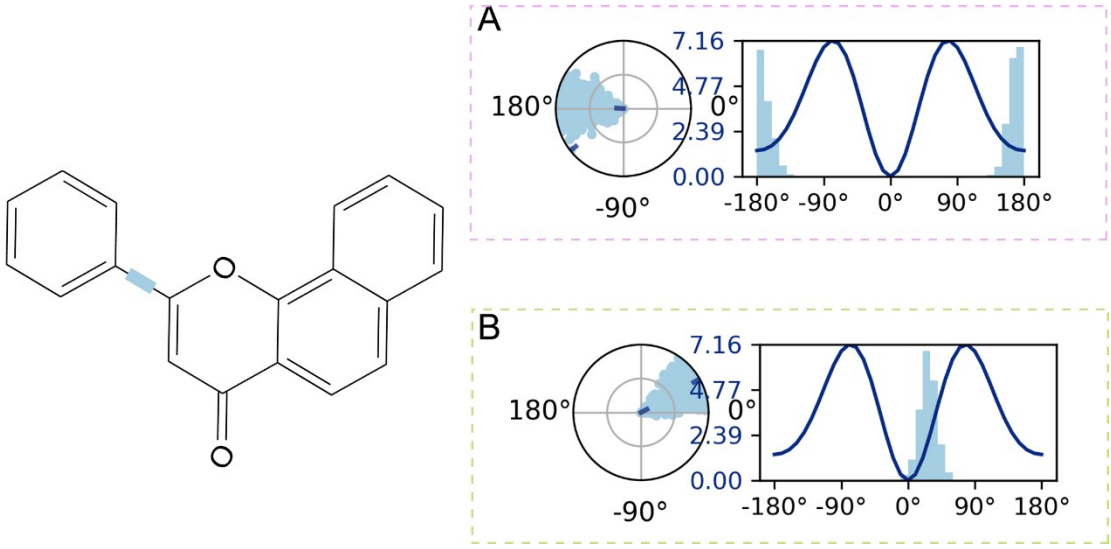

Figure S7 Conformational evolution of every rotatable bond in ANF binding with CYP1A1 (A) and CYP1B1 (B) throughout the MD simulations represented in radial plots and bar plots.

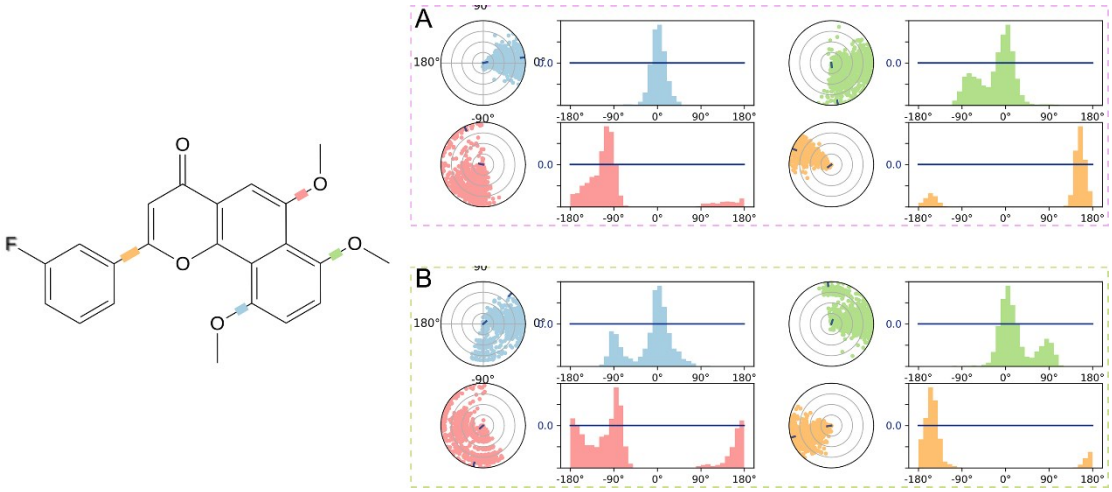

Figure S8 Conformational evolution of every rotatable bond in compound**1** binding with CYP1A1 (A) and CYP1B1 (B) throughout the MD simulations represented in radial plots and bar plots.

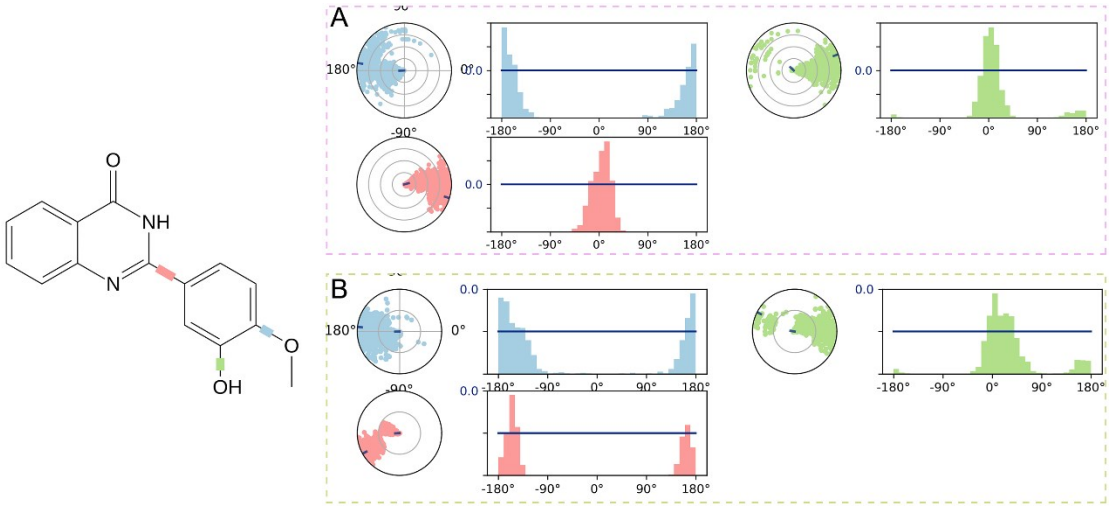

Figure S9 Conformational evolution of every rotatable bond in compound**2** binding with CYP1A1 (A) and CYP1B1 (B) throughout the MD simulations represented in radial plots and bar plots.

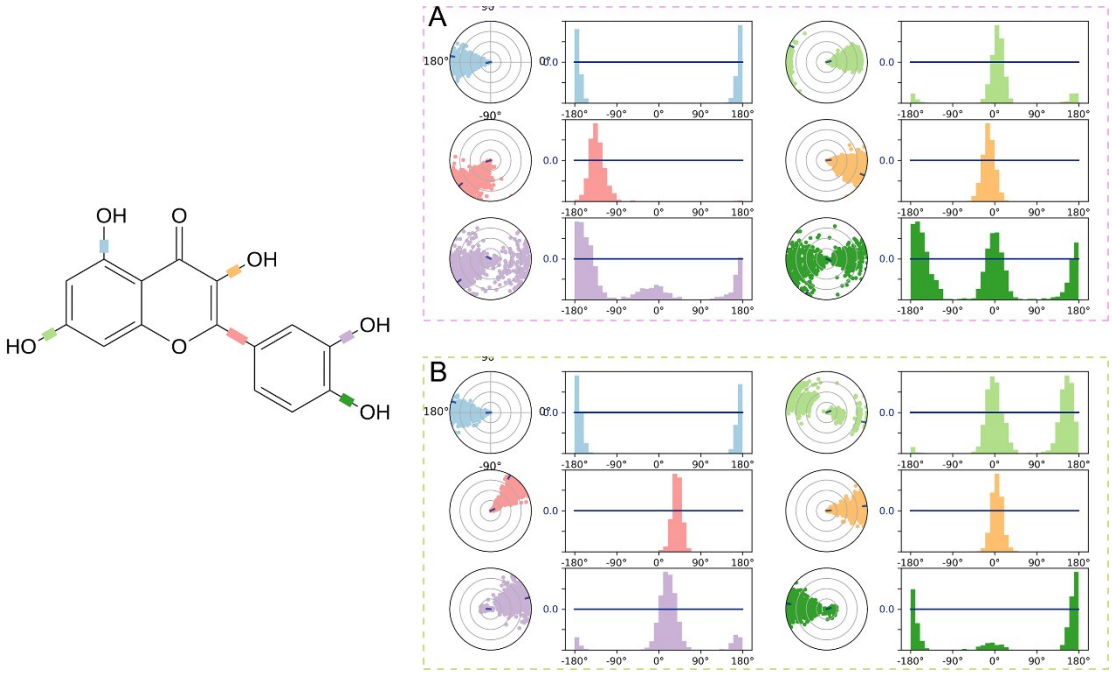

Figure S10 Conformational evolution of every rotatable bond in compound**3** binding with CYP1A1 (A) and CYP1B1 (B) throughout the MD simulations represented in radial plots and bar plots.

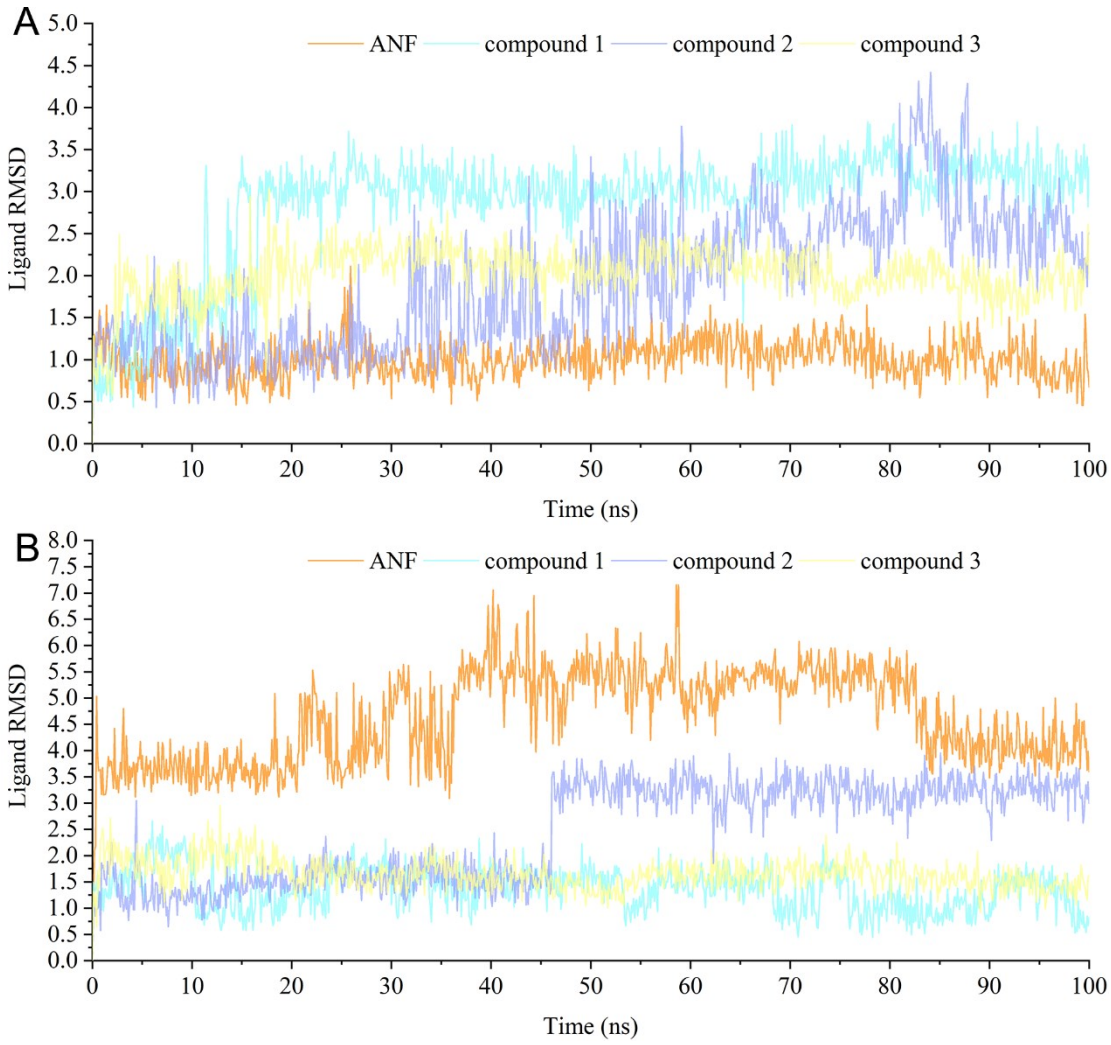

Figure S11 RMSD curves of ligand referring to protein monitored during the MD simulation. (A) CYP1A1 complexing with four inhibitors. (B) CYP1B1 complexing with four inhibitors.

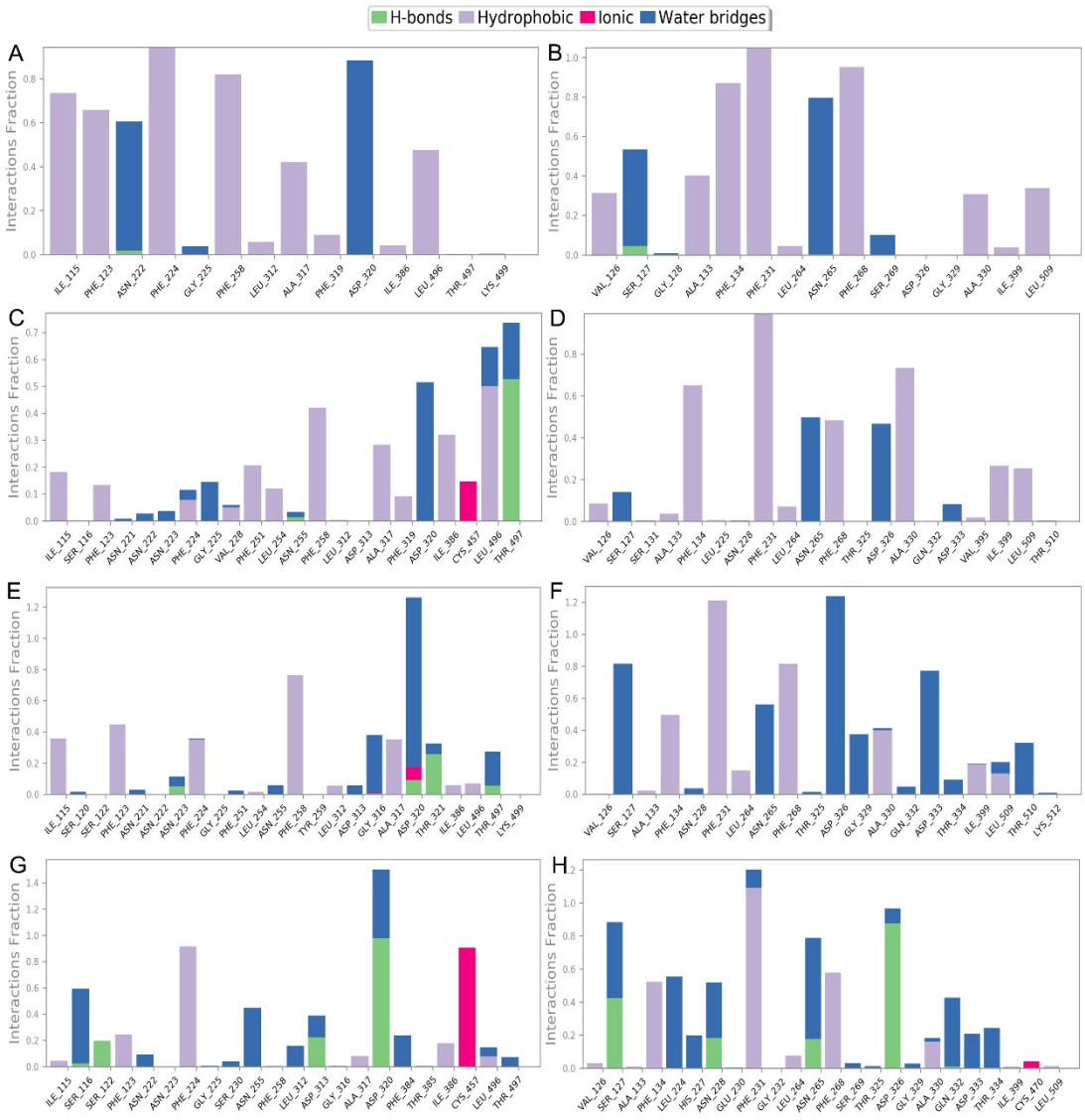

Figure S12 Fractions of protein-ligand interactions for each residue participated are monitored throughout the MD simulations. (A) CYP1A1/ANF, (B) CYP1B1/ANF, (C) CYP1A1/compound**1**, (D) CYP1B1/compound**1**. (E) CYP1A1/compound**2**, (F) CYP1B1/compound**2**, (G) CYP1A1/compound**3**, (H) CYP1B1/compound**3**.

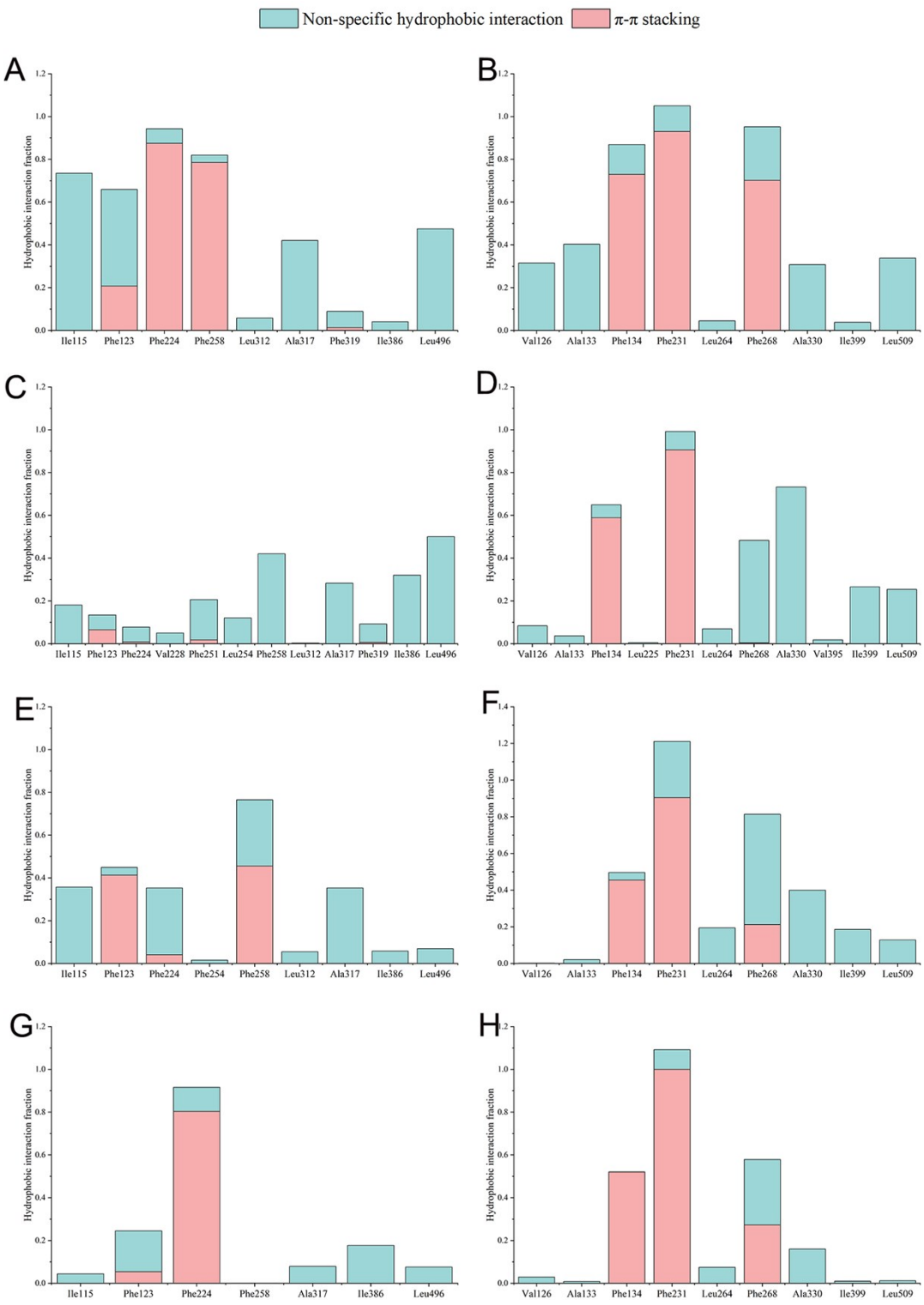

FigureS13 The fraction of hydrophobic receptor-ligand interaction of the investigated complexes during the MD simulation. (A) CYP1A1/ANF, (B) CYP1B1/ANF, (C) CYP1A1/compound**1**, (D) CYP1B1/compound**1**. (E) CYP1A1/compound**2**, (F) CYP1B1/compound**2**, (G) CYP1A1/compound**3**, (H) CYP1B1/compound**3**.

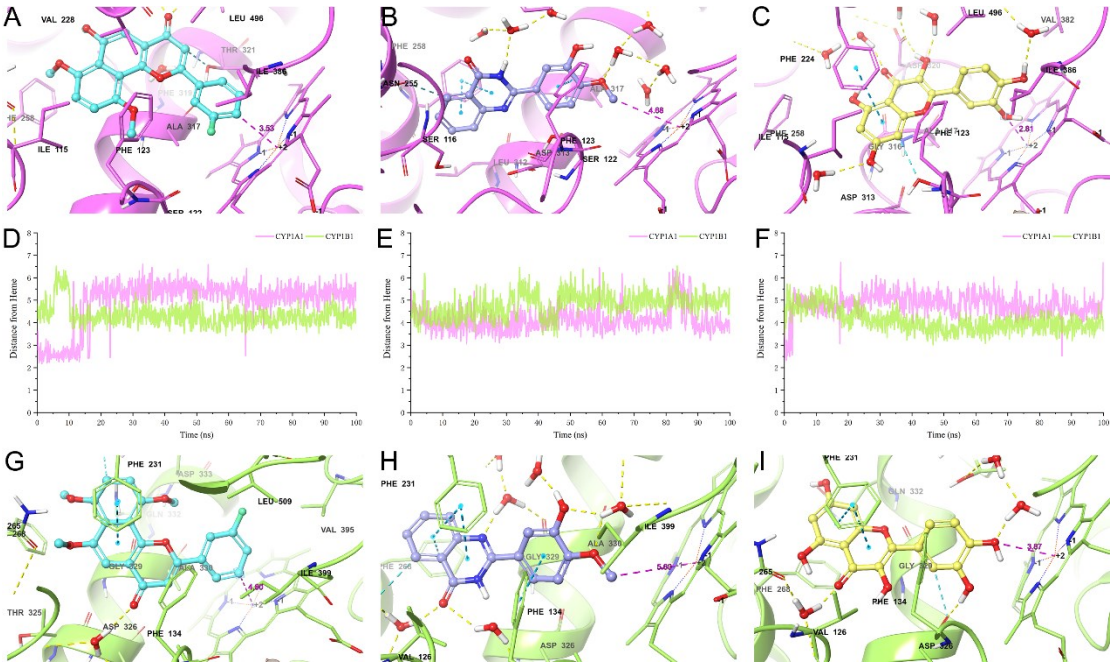

Figure S14 The atomic distance between the selective inhibitors and the iron ion of heme monitored during the MD simulations. (A) The system formed by CYP1A1 and compound**1**. (B) The system formed by CYP1A1 and compound**2**. (C) The system formed by CYP1A1 and compound**3**. (D) Distance between compound**1** and heme in CYP1A1 and CYP1B1 monitored along with the MD simulation. (E) Distance between compound**2** and heme in CYP1A1 and CYP1B1 monitored along with the MD simulation. (F) Distance between compound**3** and heme in CYP1A1 and CYP1B1 monitored along with the MD simulation. (G) The system formed by CYP1B1 and compound**1**. (H) The system formed by CYP1B1 and compound**2**. (I) The system formed by CYP1B1 and compound**3**.

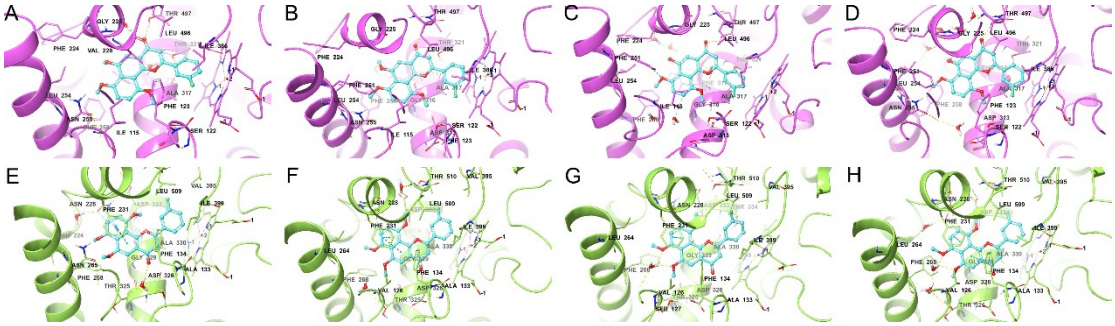

Figure S15 Representative receptor-ligand interactions between compound**1** with CYP1A1 and CYP1B1 revealed by MD trajectory clustering analysis. (A) Cluster 1 for CYP1A1/compound**1** complex, (B) Cluster 2 for CYP1A1/compound**1** complex, (C) Cluster 3 for CYP1A1/compound**1** complex, (D) Cluster 4 for CYP1A1/compound**1** complex, (E) Cluster 1 for CYP1B1/compound**1** complex, (F) Cluster 2 for CYP1B1/compound**1** complex, (G) Cluster 3 for CYP1B1/compound**1** complex, (H) Cluster 4 for CYP1B1/compound**1** complex.

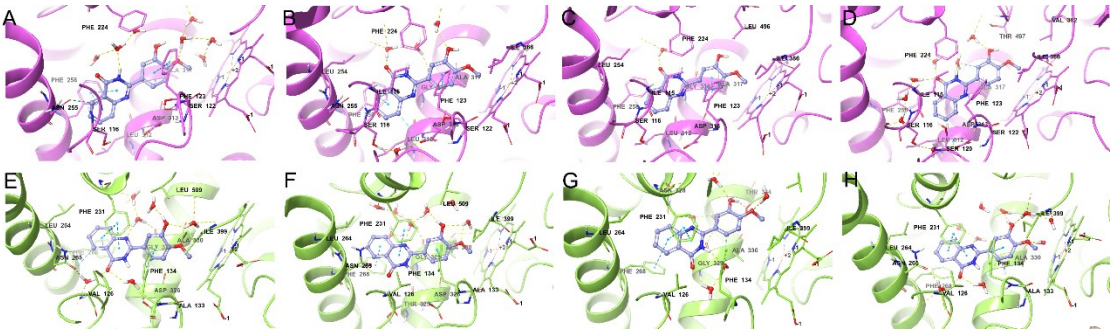

Figure S16 Representative receptor-ligand interactions between compound**2** with CYP1A1 and CYP1B1 revealed by MD trajectory clustering analysis. (A) Cluster 1 for CYP1A1/compound**2** complex, (B) Cluster 2 for CYP1A1/compound**2** complex, (C) Cluster 3 for CYP1A1/compound**2** complex, (D) Cluster 4 for CYP1A1/compound**2** complex, (E) Cluster 1 for CYP1B1/compound**2** complex, (F) Cluster 2 for CYP1B1/compound**2** complex, (G) Cluster 3 for CYP1B1/compound**2** complex, (H) Cluster 4 for CYP1B1/compound**2** complex.

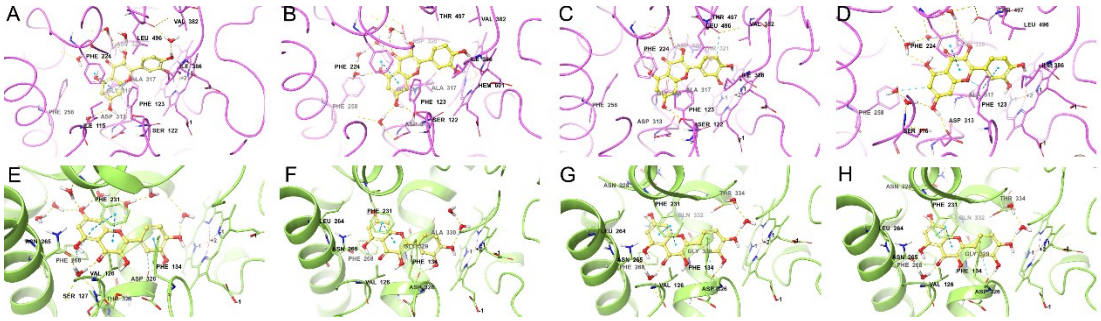

Figure S17 Representative receptor-ligand interactions between compound**3** with CYP1A1 and CYP1B1 revealed by MD trajectory clustering analysis. (A) Cluster 1 for CYP1A1/compound**3** complex, (B) Cluster 2 for CYP1A1/compound**3** complex, (C) Cluster 3 for CYP1A1/compound**3** complex, (D) Cluster 4 for CYP1A1/compound**3** complex, (E) Cluster 1 for CYP1B1/compound**3** complex, (F) Cluster 4 for CYP1B1/compound**3** complex, (G) Cluster 3 for CYP1B1/compound**3** complex, (H) Cluster 4 for CYP1B1/compound**3** complex.

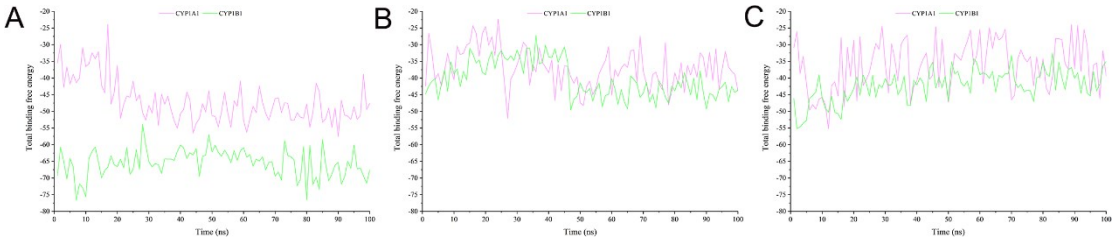

Figure S18 Time evolution of the binding free energy for the investigated compounds complexing with CYP1A1 and CYP1B1. (A) Compound**1**, (B) Compound**2**, (C) Compound**3**.